IEICE TRANS. ELECTRON., VOL.E107–C, NO.10 OCTOBER 2024

INVITED PAPER *Special Section on Microwave and Millimeter-Wave Technologies*

NRD Guide as a Transmission Medium Launched from Japan at Millimeter-Wave Frequency Applications

Futoshi KUROKI[†a)], ***Senior Member***

SUMMARY Nonradiative dielectric waveguide is a transmission medium for millimeter-wave integrated circuits, invented in Japan. This transmission line is characterized by low transmission loss and non-radiating nature in bends and discontinuities. It has been actively researched from 1980 to 2000, primarily at Tohoku University. This paper explains the fundamental characteristics, including passive and active circuits, and provides an overview of millimeter-wave systems such as gigabit-class ultra-high-speed data transmission applications and various radar applications. Furthermore, the performance in the THz frequency band, where future applications are anticipated, is also discussed.

key words: *millimeter-waves, THz waves, integrated circuits, system applications*

1. Introduction

With the commencement of 5G deployment, the nature of communication has evolved from the conventional era of person-to-person interactions to new forms such as group-to-group, group-to-device, and device-to-device. As society undergoes continuous digitization, the communication speed and the number of multiple access will be expected to increase by several tens of times compared to those of 5G because the global proliferation of IoT devices and the AI market will be expected to expand [1]. In anticipation of these trends, research on Beyond 5G has become increasingly active, particularly as we move towards the 2030s [2]–[4]. Frequencies such as millimeter and submillimeter waves, where there are currently few users, are expected to play a crucial role in facilitating these new communication technologies [5].

The nonradiative dielectric waveguide (NRD guide) was invented as a transmission medium for millimeter-wave integrated circuits in 1981 by Professor Tsukasa Yoneyama of Institute of Electrical Communication, Tohoku University envisioning their novel types of applications [6]–[8]. As illustrated in Fig. 1, research on NRD guides has been vigorously conducted both domestically and internationally over the 43-year period from 1981 to 2023, with 241 publications featured in the IEEE Explorer® Digital Library.

This paper provides a comprehensive review of NRD guides, covering fundamental aspects to applied systems, and discusses the potential utilization of the THz frequency band in the future.

Manuscript received January 14, 2024.
Manuscript revised February 22, 2024.
Manuscript publicized April 12, 2024.
[†]NIT, Kure College, Kure-shi, 737–8506 Japan.
a) E-mail: kuroki@kure.kosen-ac.jp
DOI: 10.1587/transele.2024MMI0006

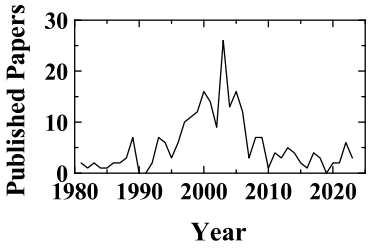

Fig. 1 Number of papers regarding NRD guide as included in IEEE Explorer® Digital Library during 43 years from 1981 to 2023.

2. Operation Principle of NRD Guide

2.1 Principle of Operation of Non-Radiating Nature [6]–[9]

Figure 2 shows typical structure of the NRD guide which consists of dielectric strips inserted in a parallel metal plate waveguide.

In a parallel metal plate waveguide, whose spacing is set at half a free space wavelength, electromagnetic wave having the magnetic wall boundary condition at the horizontally symmetric plane cannot propagate. For example, assuming an operating frequency of 60 GHz and the spacing of 2.25 mm between parallel plates, the dispersion curve of the parallel metal plate waveguide is shown by the dotted curve in Fig. 3. In the frequency range below 65.5 GHz, transmission modes cannot propagate in cutoff nature.

Inserting dielectric strips into such parallel metal plate waveguide, as shown in Fig. 2, the cutoff condition is eliminated and electromagnetic waves can propagate along the dielectric strip. When PTFE with a relative permittivity of 2.04 having low loss nature in millimeter frequencies is used as an example of dielectric strips, the dispersion curve of the NRD guide with a height of 2.25 mm and a width of 2.5 mm, respectively, is depicted by the solid curve in Fig. 3. In the frequency range above 55 GHz, electromagnetic waves become transmittable. Unwanted radiation waves generated at bends and discontinuities, as observed in conventional dielectric circuits, are suppressed in NRD guide because the locations of their occurrence are within the parallel metal plates, as indicated by the dispersion characteristics in Fig. 3. This illustrates the principle of non-radiating nature of the NRD guide.

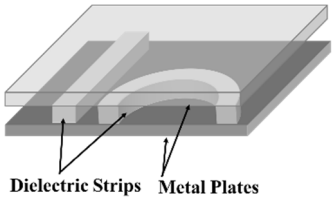

Fig. 2 Typical structure of NRD guide.

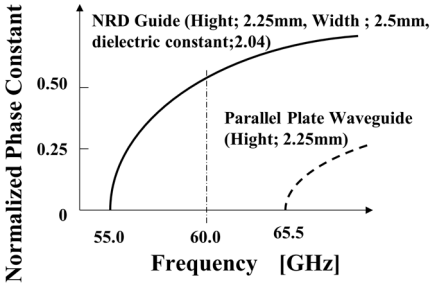

Fig. 3 Typical dispersion curves of NRD guide and parallel metal plate waveguide.

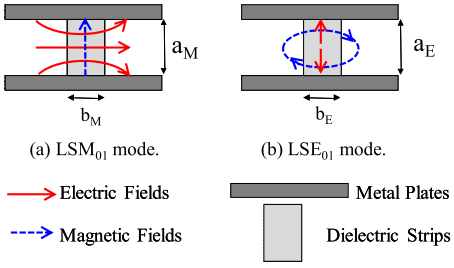

Fig. 4 Rough sketched field distributions of non-radiating modes in NRD guide.

2.2 Operational Modes

As shown in Fig. 4, the modes of the NRD guide can be classified into LSM_{01} and LSE_{01} modes, respectively, the former being characterized by magnetic fields in parallel to air-dielectric interfaces and the latter having electric fields in parallel to those interfaces [10].

The cutoff frequency of the LSE_{01} mode is lower than that of the LSM_{01} mode. However, when using low permittivity materials with a relative permittivity of 2 to 3 for the dielectric strips, the LSM_{01} mode is chosen as the operating mode for the ease of constructing functional circuit elements and the LSE_{01} mode is regarded as the parasitic mode [11]. The LSE_{01} mode is then removed using a mode suppressor, as mentioned later.

In contrast, when using high permittivity materials with a relative permittivity of 10 or more for the dielectric strips, the LSE_{01} mode is convenient as the operating mode due to its ability to create broadband performance and simple radiators [12].

The dimensions of the NRD guide for LSM_{01} mode using dielectric strips with a relative permittivity of around 2-3 are generally designed by

$$0.37 < \frac{a_M}{\lambda_0} < 0.5 \tag{1a}$$

$$0 < \sqrt{\varepsilon_M - 1}\frac{b_M}{\lambda_0} < 1 \tag{1b}$$

And those for LSE_{01} mode using dielectric strips with a relative permittivity of around 10-30 are generally designed by

$$0.16 < \frac{a_E}{\lambda_0} < 0.5 \tag{2a}$$

$$0 < \sqrt{\varepsilon_E - 1}\frac{b_M}{\lambda_0} < 1 \tag{2b}$$

where the suffixes "M" and "E" correspond to the NRD guides with LSM_{01} and LSE_{01} modes, respectively [13].

In this paper, unless specifically stated otherwise, the various characteristics of the NRD guide with the LSM_{01} mode as the operating mode will be explained.

2.3 Transmission Loss [14]

The current on the metal plate, induced by the LSM_{01} mode, is distributed entirely in the transverse direction. This behavior is similar to that of the TE_{0n} circular waveguide mode with the loss characteristics, where the conductor losses decrease with increasing frequency [15]. Therefore, by constructing the dielectric strip with low-loss dielectric materials, low-loss characteristics of the NRD guide can be ensured. The PTFE is commonly used as the dielectric material, and when copper is used as the metal plate, the transmission loss is 4 dB/m at 50 GHz. In practice, to ensure robustness, rigid aluminum is often used as the metal plate, but even in this case, the transmission loss is 6 dB/m, representing a significant improvement in losses compared to printed transmission lines.

2.4 Bend [16], [17]

Within the NRD guide bend, mode coupling [18] occurs between the operating LSM_{01} mode and parasitic LSE_{01} mode. As the LSM_{01} mode is input into the bend, a portion of its energy is converted into the LSE_{01} mode during propagation through the bend. Furthermore, as this LSE_{01} mode further propagates through the bend, the energy is converted back to the original LSM_{01} mode.

Therefore, in the design of NRD guide bends, when using the bend individually, efforts are made to ensure that only the LSM_{01} mode is converted at the output port. Alternatively, when using the bend for directional couplers or similar components, the curvature radius of the bend is designed to ensure that only the LSM_{01} mode is converted at the coupling point and the output port of the bend.

2.5 LSE_{01} Mode Suppressor [19]

The LSE_{01} parasitic mode often occurs not only within the

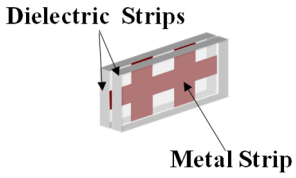

Fig. 5 Structure of LSE_{01} mode suppressor.

bend but also when the symmetry of the circuit structure is compromised. To suppress this, a mode suppressor, as shown in Fig. 5, has been devised. It is a pattern of copper foil etched on a thin dielectric substrate. By inserting it on the vertical symmetry plane of parallel metal plates, it has no impact on the LSM_{01} mode but effectively suppresses only the LSE_{01} mode. During this process, there may be propagation of TEM mode between the copper foil and the parallel metal plates, but this can be eliminated with a $\lambda/4$ choke pattern. The mode suppressor with a 5-stage choke circuit can reduce the impact of the parasitic modes to larger than 30 dB [20].

3. Passive Circuit Components of NRD Guide

3.1 Band-Pass Filter [21]–[23]

The bandpass filter is utilized for the processing of unnecessary image signals in the upconverter, as well as to ensure RF and LO isolation in the downconverter, as mentioned later. Figure 6 illustrates the structure of the cutoff guide supporting bandpass filter, where circular ceramic resonators with an unloaded Q of approximately 4000 at 60 GHz is inserted on the horizontal symmetry plane of the parallel metal plates. The cutoff guide was made of a 1 mm thick PTFE piece. This structure securely fixes the ceramic resonator within the cutoff guide. The diameter of the circular ceramic resonator was set at 2.5 mm, considering using at 60 GHz frequency bands.

The resonance modes, $EH_{21\delta}$, $TE_{02\delta}$, and $EH_{31\delta}$, were confirmed for this resonator, considering its thickness. However, for narrowband filter application, the $TE_{02\delta}$ mode, which is suitable for narrowband filters, was selected [24], [25]. As mentioned later, to design filters with center frequencies of 59 GHz and 60 GHz, the thickness of the ceramic resonator was set to 0.404 mm and 0.385 mm, respectively.

Based on the calculated coupling coefficients and load Q from the filter design, the coupling intervals for each filter, when specified as shown in Table 1, are illustrated in Figs. 7 (a) (b). Figure 7 (c) shows the calculated scattering parameters as dotted curves and the measured ones as solid curves versus frequency. The trend of the calculated and measured results closely aligns. Notably, the outstanding performance is in terms of insertion loss, with values within the passband being remarkably low at 0.3 dB and 0.5 dB for the 59 GHz and 60 GHz at center frequencies, respectively. This is largely attributed to the low-loss characteristics of the NRD guide [26].

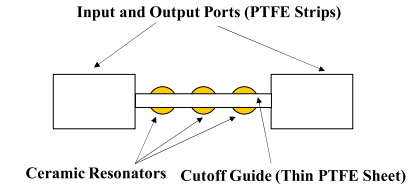

(a) Plane view

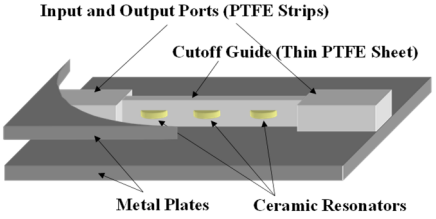

(b) Overall view

Fig. 6 Structure of bandpass filter using ceramic discs embedded in cutoff guide made by PTFE.

Table 1 Specification of evanescent-coupled bandpass filter using ceramic disk resonators.

Center frequency	59 GHz	60 GHz
Bandwidth	400 MHz	
Filter response	0.5dB ripple Chebychev	
Number of resonators	2 stages	3 stages
Diameter of ceramic resonator	2.5 mm	
Thickness of ceramic resonator	0.404 mm	0.385 mm
Resonant mode	$TE_{02\delta}$	

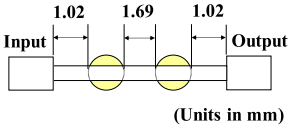

(a) Dimensions of coupling spacings in bandpass filter with bandwidth of 400 MHz at center frequency of 59 GHz.

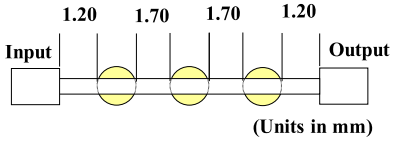

(b) Dimensions of coupling spacings in bandpass filter with bandwidth of 400 MHz at center frequency of 60 GHz.

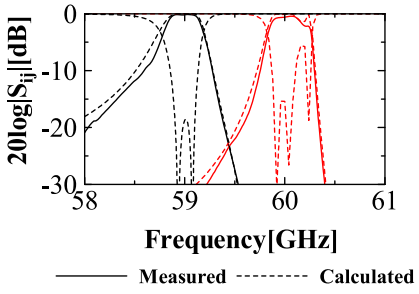

(c) Measured S parameters versus frequency.

Fig. 7 Two types of bandpass filters.

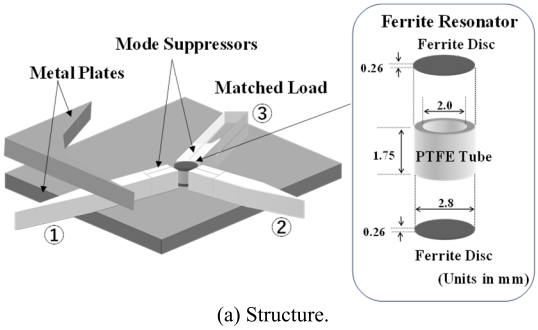

(a) Structure.

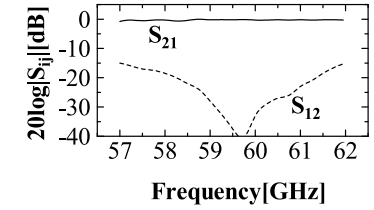

(b) Measured S parameters versus frequency.

Fig. 8 Circulator.

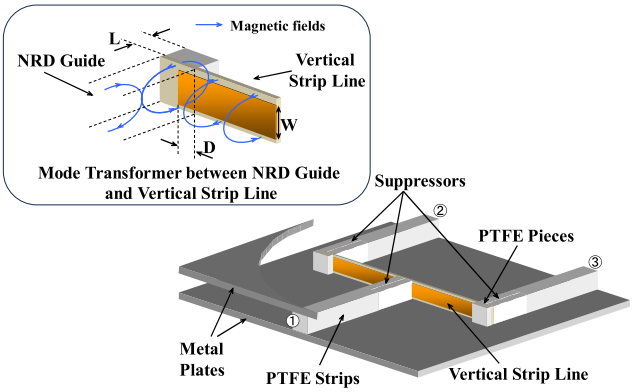

(a) Structure.

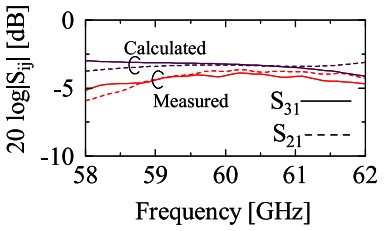

(b) Calculated and measured S parameters versus frequency.

Fig. 9 LSM$_{01}$-vetical strip line T-junction.

3.2 Circulator [19], [27], [28]

The structure of the NRD guide circulator is illustrated in Fig. 8 (a). In order to maintain symmetry in the circuit structure with respect to the horizontal symmetry plane, where the magnetic field of the LSM$_{01}$ mode is strongest and to prevent the generation of unnecessary radiation waves, two ferrite disk resonators are closely adhered to the upper and lower metal plates. PTFE tubes are inserted between the ferrite disks for support, and dielectric strips are arranged in a Y-shape around the resonator center. When a DC magnetic field is applied perpendicular to the ferrite disks in this configuration, circular operation is achieved. NiZn, with a high saturation magnetic flux density of 5 kGauss and broad bandwidth characteristics, is used as the ferrite material.

Figure 8 (b) shows the insertion loss and isolation of the prototype 60 GHz circulator. The 20 dB isolation bandwidth was measured at 3 GHz, and the insertion loss within the bandwidth was 0.5 dB or less, demonstrating performance comparable to commercially available hollow metal waveguide circulators.

3.3 Junction [29], [30]

The vertical strip line consists of a metal strip etched on a dielectric substrate which is inserted vertically into the parallel metal plate waveguide. The dominant mode is the TEM wave as shown in the inset figure of Fig. 9 (a). The field distribution of the LSM$_{01}$ mode in the cross-sectional plane resembles that of the TE$_{01}$ mode in the hollow rectangular metal waveguide, while that of the vertical strip line is similar to the coaxial line mode. A mode transformer between the NRD guide and vertical strip line can be therefore constructed by making a right-angle corner. To reduce the reflection from the mode transformer, a dielectric piece with a length of L is installed behind the right-angle corner and a metal strip is inserted between the dielectric strip and dielectric piece at a depth of D. Because a difficulty encountered in the NRD guide mode transformer and junction circuits is generation of the parasitic LSE$_{01}$ mode, the mode suppressor is installed between the NRD guide and vertical strip line to overcome such difficulty.

Figure 9 (a) shows the fabricated 3-port junction circuit. The calculated and measured scattering parameters are shown in Fig. 9 (b). Well-balanced output levels of 4 ± 0.5 dB were obtained in a bandwidth of 2 GHz at a center frequency of 60 GHz.

4. Active Circuit Components of NRD Guide

4.1 Gunn Oscillator [31]–[36]

Figure 10 (a) illustrates the structure of a self-injection locked Gunn oscillator with two output ports. The Gunn diode is horizontally inserted into a metal block with a $\lambda/4$ choke structure, and its oscillation power is guided to the NRD guide through a vertical strip resonator. To stabilize the oscillation frequency, low-loss ceramic resonators are placed behind the vertical strip resonator through a gap of spacing g. Additionally, to output the oscillation power on the Port 2 side, another NRD guide is placed behind the ceramic resonator through the same gap of spacing g. The measured oscillation powers at both ports are shown in Fig. 10 (b). With a gap spacing of 1.5 mm, both output ports achieve sufficient output level, approximately 10 dBm, suitable for

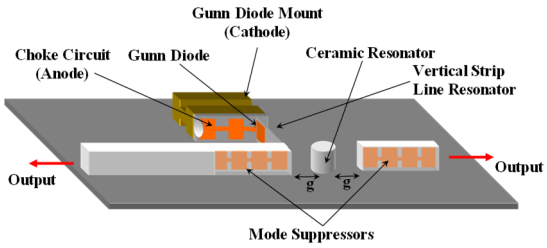

(a) Structure.

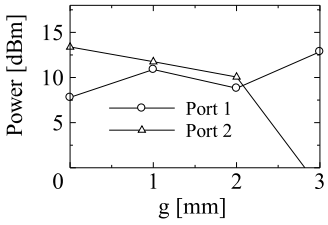

(b) Measured oscillation power.

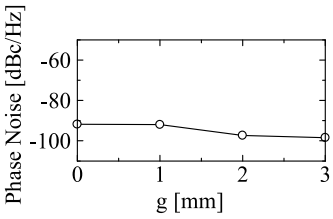

(c) Measured phase noise for 100kHz offset.

Fig. 10 Gunn oscillator with two output ports.

radar applications and local oscillation waves of frequency converters. Furthermore, the measured results of phase noise are shown in Fig. 10 (c), where at a 100 kHz offset, the value is below 95 dBc/Hz, indicating sufficiently low phase noise.

4.2 Beam Lead Diode Mount [37]–[39]

Beam-lead mount structure consisting rectangular electrodes etched on the dielectric substrate in Fig. 11. To suppress leakage of millimeter waves, a $\lambda/4$ choke is patterned onto the dielectric substrate. This structure is then adhered to the end face of the dielectric strip to serve as the mount. The beam lead diode is bonded across a 0.1 mm gap between the electrodes, and base band signals and bias lines are led externally through a coaxial line.

For diode matching, a high permittivity thin sheet is adhered just before the electrode, and to achieve complete matching, a gap is provided in the dielectric strip as a reactance element.

4.3 Frequency Converters [40], [41]

The upconverter is configured with two beam-lead diode mounts loaded with a circulator, a 3 dB coupler, and Schottky barrier diodes (SBD) (Agilent GaAs SBD: HSCH-9101), as shown in Fig. 12 (a). In this setup, a millimeter wave at a frequency of 59 GHz with a power of 10 dBm is applied

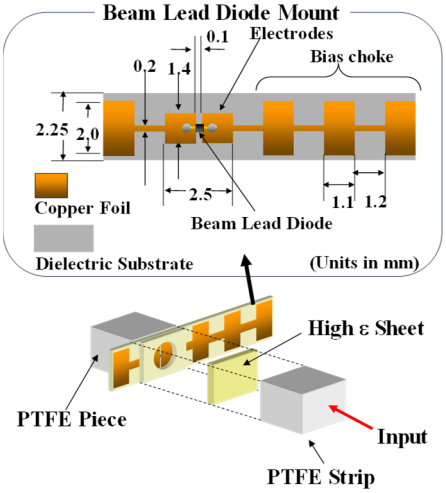

Fig. 11 Structure of beam lead diode mount.

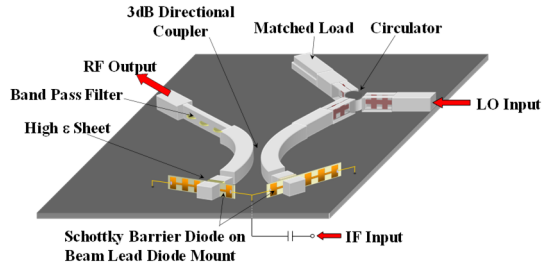

(a) Structure of up converter.

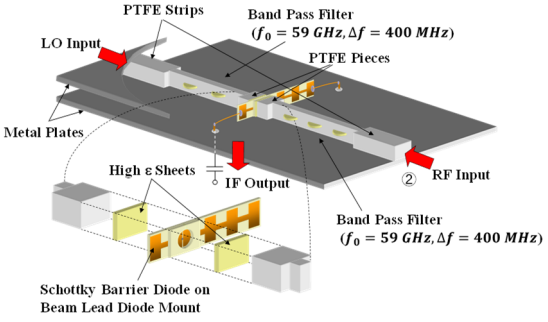

(b) Structure of down converter.

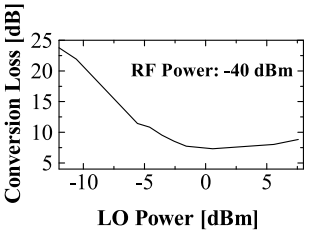

(c) Measured conversion loss versus LO power.

Fig. 12 Frequency converters.

from one port of the circulator, and a 1 GHz intermediate frequency (IF wave) is applied from the back surface of the lower metal plate through a microstrip circuit. By inputting these signals into the SBDs, upper and lower sideband images

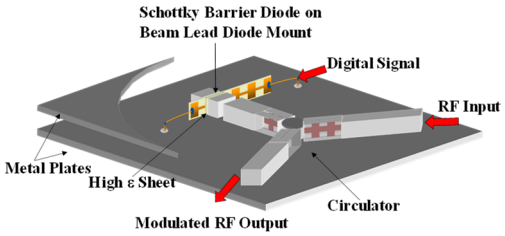

(a) Structure.

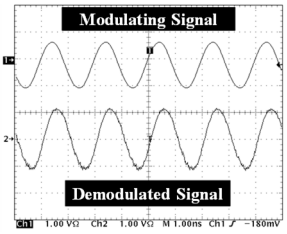

(b) Measured modulating and demodulated waveform with 1 Gbps clock.

Fig. 13 ASK modulator.

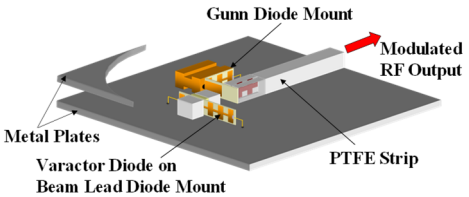

(a) Structure.

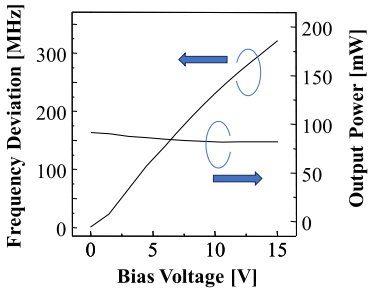

(b) Measured oscillation frequency and output power versus bias voltage.

Fig. 14 FM Gunn oscillator.

at 60 GHz and 58 GHz are generated. However, by loading the 60 GHz bandpass filter as shown in Fig. 7 (b) on the output side, the lower sideband is blocked, and only the 60 GHz millimeter wave is output. The millimeter wave output power is approximately 0 dBm when an IF power of about 12 dBm is applied.

The conversion loss at this upconverter is 12 dB, which is worse than that of the downconverter described below. This is because the upconverter operates the SBDs in the region where the output is saturated, i.e., the large signal operation region.

The structure of a single downconverter is shown in Fig. 12 (b). Two types of bandpass filters mentioned in Fig. 7 (c) are installed on both sides of a single SBD mount. Here, the LO wave at 60 GHz is input to Port 1, and the RF wave at 59 GHz is input to Port 2. As shown in Fig. 7 (c) the isolation between each bandpass filter is above 30 dB, ensuring sufficient isolation between the LO wave and RF wave. Figure 12 (c) shows the measured conversion loss of the single downconverter versus LO wave power. At an LO wave power of around 0 dBm, the conversion loss is minimized at 7 dB.

4.4 Modulators

In conventional ASK (Amplitude Shift Keying) modulators, PIN diodes are commonly used as millimeter-wave switching elements [42]. However, for modulating millimeter waves with digital signals at data transmission speeds reaching Gbps, there are limitations with PIN diodes. Instead, SBD, which have a shorter carrier lifetime, become advantageous. Figure 13 (a) illustrates the structure of an NRD guide ASK modulator consisting of an SBD-loaded beam-lead diode mount and a circulator. In this circuit, by ensuring that the SBD operates as a detector, the transmitted wave is absorbed by the diode during forward bias. During reverse bias, the wave reflects due to mismatch, resulting in the modulated wave being output at the output port. The ON/OFF characteristics of the ASK modulator designed at 60 GHz cover a bandwidth of 1.7 GHz, providing an ON/OFF ratio of 10 dB or more. Figure 13 (b) shows the modulating and demodulated waveforms at a clock rate of 1 Gb/s. While some jitter is observed, there is no significant difference between the two waveforms, indicating that this approach is a powerful ASK modulator for ultra-high-speed data transmission [43]–[45].

The structure of the NRD guide FM Gunn oscillator at 60 GHz is shown in Fig. 14 (a). The beam-lead type varactor diode for frequency modulation is implemented on the beam lead diode mount, similar to the SBD, and inserted into the dielectric strip section of the NRD guide. Additionally, this modulator is electromagnetically coupled to the Gunn oscillator through a gap, and the modulation sensitivity is determined by factors such as the length of the gap. Figure 14 (b) illustrates the oscillation output and frequency variation of the FM Gunn oscillator versus the bias voltage applied to the varactor diode. The output for a bias voltage from 0 V to 15 V is 85 ± 5 mW, and the modulation sensitivity is 21.7 MHz/V [46].

4.5 MMIC Amplifier

The electromagnetic field of the NRD guide spreads around the dielectric strip. On the other hand, the field of the microstrip line is concentrated between the ground conductor and the central conductor, making direct connection between the two lines challenging. To address this, an NRD guide-microstrip line transformer, as shown in Fig. 15 (a), has been devised using a vertical strip line and a coaxial line that is easily connectable to the microstrip line.

The microstrip line has its central conductor supported by a ground plate, positioned on the horizontal symmetry

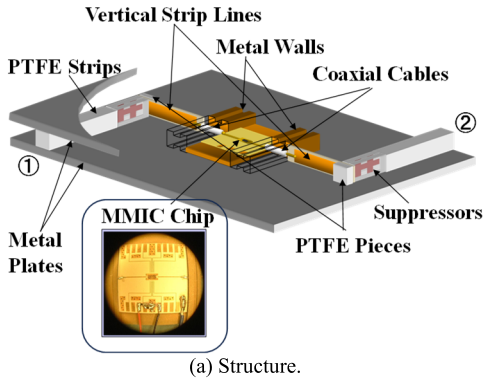

(a) Structure.

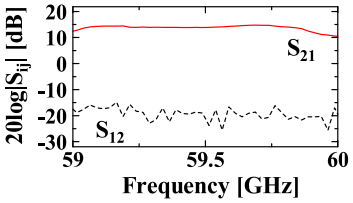

(b) Measured scattering parameters.

Fig. 15 MMIC amplifier.

plane of the parallel metal plate. The central conductor of the microstrip line is connected to the central conductor of a coaxial line formed within a metal piece with the same height as the parallel metal plate spacing. This metal piece is strategically placed to prevent unwanted radiation waves generated by the microstrip line. To suppress electromagnetic waves leaking between the metal piece and the parallel metal plate, a $\lambda/4$ step groove choke circuit is loaded onto this metal piece [47].

Figure 15 (b) shows the characteristics of an amplifier implemented with a 0.15 μm gate length HEMT MMIC chip (TRW ALH321C) mounted on the microstrip line. The amplifier shows a forward gain of 15 dB and an average reverse isolation of −20 dB over a 1 GHz bandwidth at a center frequency of 59.5 GHz [48].

5. Applications

5.1 Giga-bit Class Data Transmission [44]

Figure 16 shows an ASK transmitter and receiver created using the aforementioned ASK modulator and other components. This device was developed by Professor Yoneyama's startup company, MMEX Corporation. It is capable of transmitting uncompressed high-definition TV signals at a transmission speed of 1.5 Gbps. This device was put into practical use along with goal cameras for ice hockey broadcasts in Sapporo.

5.2 FM-CW Radar [49]

Figure 17 (a) shows a 59.5 GHz band FM-CW radar front end with a three-layer structure. The upper layer, Layer1, consists of an oversized waveguide excited long slot array

Fig. 16 Photograph of ASK transceiver (left) and receiver (right) for distribution of uncompressed high-definition TV signal with data rate of 1.5 Gbps.

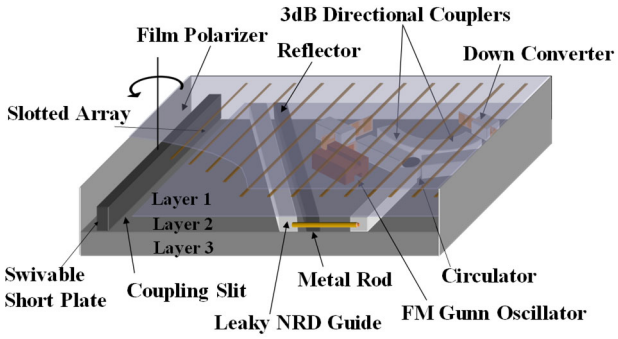

(a) Structure.

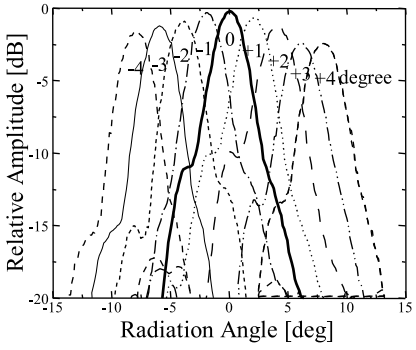

(b) Measured radiation patterns versus leaning angle.

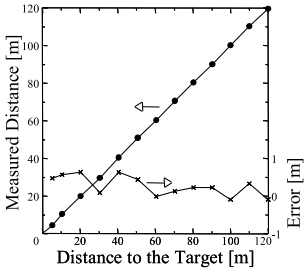

(c) Measured distance of target.

Fig. 17 FM-CW radar.

planar antenna, with a polarization conversion film provided on the top of the long slot array to convert the linear polarization plane perpendicular to the long slot to a diagonal 45 degree angle. The second layer, Layer2, is composed of an

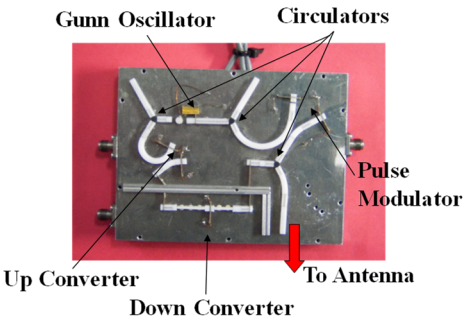

(a) Photograph of radar front-end.

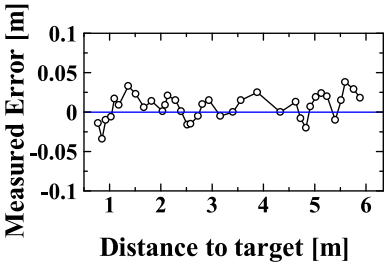

(b) Measured error versus distance to target.

Fig. 18 Pulse radar.

NRD guide FM-CW radar front-end and a leaky wave NRD guide connected through a reflecting plate. The oversized waveguide of Layer 1 is connected to the oversized waveguide of Layer 2, excited by the leaky wave NRD guide, through a coupling slit and a folding structure. As the leaky waves from the leaky NRD guide propagate diagonally forward, the guides are arranged diagonally to ensure that the propagation direction of the leaked waves is orthogonal to the long slot. The reflecting plate is provided to operate the leaked wave NRD guide as a single-direction radiating element, and a coaxial line penetrates this part, connecting the NRD guide circuit and the leaky wave NRD guide. The third layer, Layer3 contains the intermediate frequency and baseband circuits.

The short plate at the coupling slit is mechanically rotated, allowing the main beam radiation angle in the plane parallel to the slot to be scanned. Figure 17 (b) shows the measured radiation directional in the plane parallel to the slot for the rotation angle of the short plate. The main beam can be scanned from −8 degrees to +8 degrees in the range of −4 degrees to +4 degrees of the rotation angle of the short plate.

With a beam scanning frequency of 7 times per second, actual distance measurements were conducted targeting a passenger car, as shown in Fig. 17 (c). The distance measurement error in the range of 5m to 120m is below 0.7 m, and the measurement error for relative velocity is below 1 km/h.

5.3 Pulse Radar [50]

Figure 18 illustrates a millimeter wave pulse radar front-end designed for tank level sensing. The millimeter waves generated by the Gunn oscillator are split into two directions. One portion is input to a balanced ASK modulator via an isolator, and the pulse-modulated millimeter waves are radiated as RF waves by a planar antenna with a gain of 33 dBi. The reflected waves from the target object are received by the antenna and directed to the receiving circuit through the circulator as a duplexer. In the receiving circuit, an up-converter shown in Fig. 12 (a) is connected to the oscillator to obtain the LO wave for heterodyne reception. This LO wave and the reflected waves from the target object are mixed at the down converter as shown in Fig. 12 (b), resulting in a pulse-modulated 1 GHz IF signal, which is then directed to the IF/baseband unit. The distance to the tank level is measured using an FPGA (Altera Stratix: EP1S10F780C7ES). Figure 18 (b) shows the results of the ranging experiment, and the error is within ±3 centimeters.

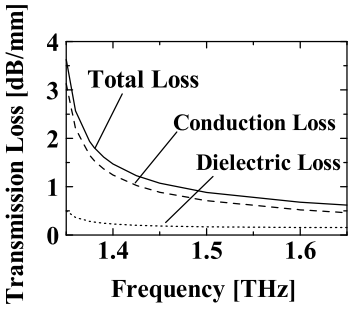

Fig. 19 Calculated transmission loss of NRD guide versus frequency.

Table 2 Comparison of calculated transmission loss between NRD guide and coplanar waveguide.

	Coplanar Waveguide	NRD Guide
Frequency	1.0 THz	1.5 THz
Transmission Loss	8.0 dB/mm	1.0 dB/mm

6. Challenge to THz Frequency Band

Assuming the dielectric material to be polyethylene with a relative dielectric constant of 2.3 due to its low loss tangent of about 10^{-4}, the cross-sectional dimensions are "a = 90 μm" and "b = 90 μm" at a center frequency of 1.5 THz.

The transmission loss, α_t, consisting of conduction loss, α_c and dielectric loss α_d, was calculated as a function of frequency and the result is shown in Fig. 19. It is obvious that the main dissipation is due to the conduction loss. Comparison between transmission losses of the NRD guide and the coplanar waveguide [51] is summarized in Table 2. From these results, the transmission loss of the NRD guide is remarkably lower than that of the coplanar waveguide [52].

7. Conclusions

This paper explains the fundamentals of the NRD guide and discusses representative passive and active circuits, as well as their applications in an uncompressed high-definition TV signal transmission system and FM-CW and pulse radar

systems. It also touches upon the advantages of NRD guides in the THz wave band.

The advantages of NRD guides include comparable performance to waveguides and the compact size achieved by integrating all circuit elements into a 2.5-dimensional single housing.

As a future theme, the establishment of mass production technology using 3D printers is mentioned. Furthermore, in the terahertz wave band where the dimensions of NRD guides are on the order of several tens of microns, manufacturing methods using etching process may also be attractive.

Expectations are high for the ongoing advancements in NRD guide technology.

Acknowledgments

The author would like to express gratitude to Dr. Masaru Sato of Fujitsu Limited and Mr. Yuki Kawahara of Kawashima Manufacturing Co., Ltd., for their valuable cooperation in summarizing this paper. Additionally, heartfelt thanks to the late Professor Tsukasa Yoneyama, Honorary Professor at Tohoku University, for his extensive guidance throughout the research on NRD guides. The author also commends the diligent efforts of the Professor's students who actively contributed to the development of NRD guides.

References

[1] https://www.soumu.go.jp/main_content/000799628.pdf
[2] https://www.soumu.go.jp/johotsusintokei/whitepaper/ja/r05/html/datashu.html#f00396
[3] chrome-extension://efaidnbmnnnibpcajpcglclefindmkaj/https://www.soumu.go.jp/johotsusintokei/whitepaper/ja/r05/pdf/n5300000.pdf
[4] N. YAMANAKA, at al. "Future Vision of Beyond 5G Network - verview of Architecture and Breakthrough Technologies for 2030 (in Japanese)," IEICE Trans., vol.J104-B, no.3, pp.315–336, 2021.
[5] H. HAMADA, et al., "300 GHz Power Amplifier and 120 Gb/s, 9.8m Wireless Transmission Based on 80-nm InP-HEMT Technology (in Japanese)," IEICE Trans., vol.J104-C no.9 pp.257–266, 2021.
[6] T. Yoneyama and S. Nishida, "Nonradiative dielectric waveguide for millimeter-wave integrated circuits," IEEE Trans. Microwave Theory and Tech., vol.29, no.11, pp.1188–1192, Nov. 1981.
[7] T. Yoneyama and S. Nishida, "Nonradiative dielectric waveguide circuit components," Infrared and millimeter waves, vol.4, pp.439–449, 1984.
[8] T. Yoneyama, "Millimeter wave integrated circuits using nonradiative dielectric waveguide (in Japanese)," IEICE Trans. (C-I), J73-C-I, no.3, pp.87–94, March, 1990.
[9] F. Kuroki, T. Wagatsuma, and T. Yoneyama, "Millimeter-wave Car Radar Based on NRD Guide Technology," Transaction on IEICE, vol.87, no.9, pp.765–769, 2004.
[10] R.E. Collin, Field Theory of Guided Waves, McGraw-Hill, 1960.
[11] T. Yoneyama, H. Tamaki, and S. Nishida, "Analysis and measurements of nonradiative dielectric waveguide bends," IEEE Trans. Microwave Theory & Tech., vol.34, no.8, pp.876–882, 1986.
[12] F. Kuroki, M. Yamaguchi, Y. Minamitani, and T. Yoneyama, "High Permittivity LSE-NRD Guide and Its Application to New Type of Millimeter Wave Antenna," IEICE Trans., vol.86-E, no.2, pp.169–175, 2003.
[13] F. Kuroki, M. Yamaguchi, Y. Wagatsuma, and T. Yoneyama, "NRD Guide Integrated Circuit-Compatible Folded Planar Antenna Fed by High Permittivity LSE-NRD Guide Radiator at 60 GHz," IEICE Trans., vol.87-E, no.9, pp.1412–1417, 2004.
[14] T. Yoneyama, N. Tozawa, and S. Nishida, "Loss measurements of nonradiative dielectric waveguide (Special Papers)," IEEE Trans. Microwave Theory & Tech., vol.32, no.8, pp.943–946, 1984.
[15] H. Wei and S. Yuecong, "Study on High Power Circular Waveguide TE0n-TE11 Mode Conversion," 2007 8th International Conference on Electronic Measurement and Instruments, pp.2-78–2-81, 2007.
[16] T. Yoneyama, M. Yamaguchi, and S. Nishida, "Bends in nonradiative dielectric waveguides," IEEE Trans. icrowave Theory & Tech., vol.30, no.12, pp.2146–2150, 1982.
[17] T. Yoneyama, H. Tamaki, and S. Nishida, "Analysis and measurements of nonradiative dielectric waveguide bends," IEEE Trans. Microwave Theory & Tech., vol.34, no.8, pp.876–882, 1986.
[18] S.P. Morgon, "Theory of curved circular waveguide containing an inhomogeneous dielectric," Bell Syst. Tech. J., vol.36, no.5, pp.1209–1251, Sept. 1957.
[19] H. Yoshinaga and T. Yoneyama, "Design and fabrication of a nonradiative dielectric waveguide circulator," IEEE Trans. Microwave Theory & Tech., vol.36, no.11, pp.1526–1529, 1988.
[20] F. Kuroki, M. Kimura, and T. Yoneyama, "Analytical Study on Guided Modes in a Vertical Strip Line Embedded in an NRD Guide," IEE Electronics Letter, vol.40, no.18, pp.1121–1122, 2004.
[21] T. Yoneyama, F. Kuroki, and S. Nishida, "Design of nonradiative dielectric waveguide filters (short papers)," IEEE Trans. Microwave Theory & Tech., vol.32, no.12, pp.1659–1662, 1984.
[22] T. Yoneyama, F. Kuroki, and S. Nishida, "Experimental Design of nonradiative dielectric waveguide filters (in Japanese)," Trans. on IECE, vol.J68-B, no.2, pp.213–219, 1985.
[23] T. Miyashita and T. Yoneyama, "50 GHz Nonradiative Dielectric Waveguide Filter Using Low Loss Ceramic Resonators (in Japanese)," Trans. on IEICE, vol.J72-C, no.10, pp.659–664, 1989.
[24] F. Kuroki, S. Shinke, T. Yoneyama , and H. Sato, "Band-Widening of Ceramic Resonator Loaded NRD Guide Band-Pass Filter at 60 GHz," IEICE Trans., vol.84-E, no.10, pp.1569–1574, 2001.
[25] F. Kuroki, Y. Murata, and T. Yoneyama, "Millimeter-wave Duplexer with Low loss and High Isolation Based on the NRD Guide Technology at 60 GHz," IEE Electronics Letter, vol.40, no.13, pp.808–810, 2004.
[26] F. Kuroki, M. Kimura, U. Murata, and T. Yoneyama, "A Compact-Sized NRD Guide Single Mixer Using Band-pass Filters at 60 GHz," Electronic Proc. IEEE Trans. Microw. Theory Techn.-S Microwave Symp., June, 2005 in Long Beach, USA, pp.2091–2094, 2005.
[27] F. Kuroki, S. Ishikawa, and T. Yoneyama, "New Type of Ferrite Resonator for NRD Guide Circulator at 60 GHz.," Proc. National Radio Science Meeting, p.88, Boulder, USA, Jan. 2006.
[28] Y. Kubo and F. Kuroki, "Calculation of NRD Guide Circulator at 94GHz," Electronic Proc. Thailand-Japan MicroWave, 2 pages, Dece. 2013 in Bangkok, Thailand, 2013,
[29] F. Kuroki, M. Kimura, and T. Yoneyama, "Fully CAD based Design of Junction circuits Using NRD Guide and Vertical Strip Line Transition at 60 GHz," IEICE Trans., vol.88-E, no.1, pp.105–109, 2005.
[30] F. Kuroki, M. Kimura, K. Yamaoka, and T. Yoneyama, "T-Junction Using NRD Guide /Vertical Strip Line Transition at 60GHz," Proc. Progress in Electromagnetics Research Symp., p.232, Jan. 2003.
[31] M. Takada and T. Yoneyama, "Self-injection Locked Gunn Oscillator Using Nonradiative Dielectric Waveguide (in Japanese)," Electron. Comm. Jpn. Pt. II, vol.72, no.11, pp.95–101, 1989.
[32] F. Kuroki, S. Ishikawa, and T. Yoneyama, "Comparative Study on Two Types of Self-Injection Locked NRD Guide Gunn Oscillators," Proc. 35th European Microwave Conference, pp.217–220, Oct. 2005.
[33] F. Kuroki and K. Ohue, "Reflection Type of Injection Locked Gunn Oscillator and Its Applications at 60 GHz," Electronic Proceedings of National Radio Science Meeting, Jan. 2008.
[34] K. Ohue, F. Kuroki, and T. Yoneyama, "Analytical Consideration on Reflection Type of Self-injection Locked NRD Guide Gunn Oscil-

lator at 60 GHz," 2009 European Microwave Conference (EuMC), pp.476–479, Oct. 2009.
[35] F. Kuroki, S. Takeda, and T. Ohira, "Numerical Analysis of Q-factors in Millimeter-wave Oscillators," Electronic Proceedings of Progress in Electromagnetics, July 2010.
[36] T. Tanaka and F. Kuroki, "Verification on Equivalent Circuit Model of Band-stop Type of Self-injection Locked NRD Guide Gunn Oscillator at 60GHz," IEEJ Transactions on Electronics, Information and Systems, vol.133, no.5, pp.966–970, May 2013.
[37] F. Kuroki and T. Yoneyama, "Nonradiative Dielectric Waveguide Components Using Beam-Lead Diodes (in Japanese)," Trans. on IEICE, vol.J73-C-I, no.2, pp.71–76, 1989.
[38] F. Kuroki, S. Shinke, T. Mukai, E. Suematsu, H. Sato, and T. Yoneyama, "Band Widening of NRD Guide Schottky Barrier Diode Devices and Its Application to a Wireless Multi-Channel TV-Signal Distribution System at 60 GHz," IEICE Trans., vol.86-E, no.12, pp.2422–2428, 2003.
[39] F. Kuroki, Y. Murata, R. Masumoto, and T. Yoneyama, "New Type of NRD Guide Beam-Lead Diode Mount at 60 GHz.," Proc. National Radio Science Meeting, p.83, Jan. 2006.
[40] F. Kuroki, M. Sugioka, H. Kawano, T. Yanatsubo, E. Suematsu, H. Sato, and T. Yoneyama, "60GHz Multi-Channel TV Signal Transmission System Based on the NRD Guide Technology ," The 10th Asia Pacific Microwave Conference, Yokohama, 1998.
[41] F. Kuroki, M. Kimura, and T. Yoneyama, "A Filter-based NRD Guide Up-converter at 60 GHz.," Proc. Topical Symposium on Millimeter-waves, pp.155–158, Feb. 2005.
[42] F. Kuroki, S. Nakamura, T. Fukuchi, and T. Yoneyama, "NRD Guide P-I-N Diode Devices for Automotive Radars at 77GHz," IEICE Trans., vol.86-E, no.2, pp.199–205, 2003.
[43] F. Kuroki, M. Sugioka, S. Matsukawa, K. Ikeda, and T. Yoneyama, "High Speed ASK Transceiver Based on the NRD-Guide Technology at 60-GHz band," IEEE Trans. Microwave Theory Tech., vol.46, no.6, pp.806–810, 1998.
[44] F. Kuroki, M. Yamaguchi, T. Araki, H. Sato, and T. Yoneyama, "Gigabit Class Ultra High Speed Signal Wireless Distribution by Using NRD Guide Technology at 60GHz," Proc. IEEE Trans. Microw. Theory Techn.-S Microwave Symp., pp.619–622, June 2003.
[45] F. Kuroki,, M. Yamaguchi, M. Sugioka, and T. Yoneyama, "Ultra High-speed Millimeter-wave Integrated Circuits Using NRD Guide (in Japanese)," IEEJ Trans. EIS, vol.124, no.2, pp.308–313, 2004.
[46] F. Kuroki, J. Baba, and T. Yoneyama, "NRD-Guide FM Gunn Oscillator at 60 GHz Band (in Japanese)," Trans. on IEICE, vol.J77-C-I, no.11, pp.592–598, 1994.
[47] F. Kuroki, M. Kimura, and T. Yoneyama, "A Transition between NRD Guide and Microstrip Line 60 GHz" IEICE Trans., vol.E88-C, no.10, pp.1968–1972, Oct. 2005.
[48] F. Kuroki, M. Kimura, and T. Yoneyama, "Fully CAD-Based Design of Mode Transformer between NRD Guide and Vertical Strip Line and Its Applications to Junction Circuits and MMIC Integration at 60GHz," Proc. 33rd European Microwave Conference, pp.555–558, Oct. 2003.
[49] F. Kuroki, Y. Wagatsuma, and T. Yoneyama, "Distance Estimation at 60 GHz," IEEE Aerospace and Electronic Systems Magazine, vol.21, no.5, pp.26–29, May 2006.
[50] F. Kuroki, K. Yamaoka, S. Ishikawa, Y. Murata, A. Izufo, and T. Yoneyama, "NRD Guide Pulse Radar for Distance Estimation at 60 GHz (in Japanese)," IEEJ Trans. EIS, vol.128, no.6, pp.825–831, 2008.
[51] M.Y. Frankel, S. Gupta, J.A. Valdmanis, and G.A. Mourou, "Terahertz Attenuation and Dispersion Characteristics of Coplanar Transmission Lines," Trans. on IEEE Microwave Theory and Techniques, vol.39, no.6, pp.910–916, 1991.
[52] F. Kuroki, H. Ohta, and T. Yoneyama, "Transmission Characteristics of NRD Guide as a Transmission Medium in THz Frequency Band," Proc. Joint 30th International Conference on Infrared and Millimeter Waves and 13th International Conference on Terahertz Electronics, vol.2, pp.331–332, Sept. 2005.

Futoshi Kuroki received the associate B.E. degree in electrical engineering from Kure National College of Technology, Japan, in 1980, the B.E. degree in electronics engineering from Kyusyu Institute of Technology, Japan, in 1982, and the M.E. and Ph.D. degrees in electrical communication engineering from Tohoku University, Sendai, Japan, in 1984 and 1987, respectively. From 1987 to 1995, he was a Research Associate at the Research Institute of Electrical Communication, Tohoku University. Since 1995, he has been with Kure National College of Technology, Hiroshima, Japan, where he is a Commissioned Professor in the Department of Electrical Engineering and Information Science. He has been engaged in research work on electromagnetic devices, circuits, antennas, and systems. Dr. Kuroki is a member of the Institute of Electronics, Information and Communication Engineering (IEICE) in Japan, the Institute of Electrical and Electronics Engineers (IEEE) in USA.